www.jcimcr.org

JCIMCR OPEN ACCESS Journal of Clinical Images and Medical Case Reports

ISSN 2766-7820

Research Article

Open Access, Volume 6

Chest radiography optimization: Identifying the optimal kV for image quality in a phantom study

***Corresponding Author: Ioannis Antonakos**

Department of Radiology, National and Kapodistrian University of Athens, 1st Rimini St., Chaidari, 12461 Athens, Greece.

Email: iantonakos@med.uoa.gr

Received: Oct 07, 2025

Accepted: Nov 05, 2025

Published: Nov 12, 2025

Archived: www.jcimcr.org

DOI: www.doi.org/10.52768/2766-7820/3833

Abstract

Introduction: The aim of the present study was to conduct a quantitative assessment for the optimization of chest radiography acquisition protocols in order to enhance image quality, while minimizing patient radiation exposure.

Materials & methods: Measurements were conducted using a digital radiography system (AGFA DR 600). Exposures were acquired at three tube voltage (kV) settings for different patients' thicknesses simulated by PMMA slabs, with Leeds TOR 15FG image quality phantom positioned centrally within the setup. Quantitative image quality evaluation was undertaken through the calculation of Signal-to-Noise Ratio (SNR) and Contrast-to-Noise Ratio (CNR) derived from Mean Pixel Values (MPVs) for each image. Radiation dose was assessed by determining the Entrance Surface Dose (ESD).

Results: For thicknesses that attribute to average and obese patients, performance indices normalized to dose (CNR2·SNR/ESD) were higher for 115 kV and 121 kV, respectively. For slim patients the same index was higher for 104 kV.

Discussion: Results demonstrated a systematic dependence of both image quality and dose on the selection of tube voltage and phantom thickness. Optimization metrics combining CNR and SNR normalized to dose indicated better image quality in agreement with dose for a voltage selection 5kV lower than the protocol used in the clinic, for slim and average patients.

Conclusion: Further optimization of exposure parameters may be needed for the improvement of image quality while ensuring that patient dose remains as low as reasonably achievable. However, validation through clinical images evaluation is essential for the alternation of the routine in radiographic practice.

Background

According to International Atomic Energy Agency chest radiography is the most commonly requested diagnostic procedures across all age groups [1-3]. As indicated by Kamposioras et al. a cross-sectional study carried out in highly populated areas of Greece found that 20% of Greek adults had undergone the procedure at least once over the past three years, and nearly half of them (48%) reported doing so as frequently as once every three years or more [4]. In another survey conducted by Proiskos et al. among 211 physicians in Greece, 88% stated that they recommend chest radiography for early diagnosis, with 78% doing so during routine check-ups and 77% as part of cancer screening [5].

A radiograph depicts the spatial arrangement of tissue elements through differences in optical density. The quality of the image can be quantified in terms of contrast, sharpness (or resolution), and noise level. Contrast results from the variations in the extent of X-ray absorption by the various tissues, sharpness corresponds to the amount of resolution of fine detail, and noise consists of the random variations in the image which

blur the fine detail. Accurate evaluation and diagnosis depend on the ability to distinguish structures of interest from the surrounding background [4].

While the dose of radiation from a single chest X-ray is generally considered low [6,7], the large number of examinations performed, as well as the repeated use of chest X-rays in individual patients [5,8-11] can cause a significant cumulative exposure [12]. The Medical use of ionizing radiation is globally recognized as fundamental to the preservation and advancement of human health; nevertheless, serves as the primary source of artificial radiation exposure. In diagnostic imaging, the fundamental aim of radiological protection is to minimize patient doses to the lowest level reasonably achievable [13], while maintaining the integrity of diagnostic results [1].

The primary dose quantity measurable for radiographic exposures is the Entrance Surface Dose (ESD). The ESD represents the radiation dose received by the skin at the point where the X-ray beam enters the body, accounting for both the incident air kerma and the radiation backscattered from tissue. It can be determined either by placing small dosimeters on the skin or by calculating it from radiographic exposure parameters combined with measurements of the X-ray tube output [4].

As discussed above, there must be a balance between quality of radiography image and dose to the patient. Consequently, there may be instances where repeated optimization of protocols is required to ensure that the patient dose is kept low while maintaining sufficiently high image quality. Traditionally, acquisition parameters have been determined based on recommendations from governing authorities, guidance from equipment manufacturers, and the radiographer's personal expertise [14]. Therefore, the aim of our study was to find a straightforward and alternative approach in optimizing radiographic acquisition parameters.

Materials & methods

In this study a digital radiography system (AGFA DR 600, Agfa-Gevaert, Belgium) [15] was utilized at Attikon University Hospital (Athens, Greece) for all measurements.

Phantom thickness for patients' categorization

To simulate different patient chest dimensions, Polymethyl Methacrylate (PMMA) slabs of varying thicknesses were employed, corresponding to slim, average, and obese patients.

The categorization was made as follows:

PMMA thickness (cm)	Patient category
14	Slim (45-55 kg)
15	
16	
18	Average (65-85 kg)
20	
22	
23	Obese (90-100kg)
24	
25	

Setup & irradiation

For each configuration, the slabs were positioned on a tray in front of the bucky, with a Leeds TOR 18FG image quality phantom placed centrally within the phantom. Initially, the standard clinic protocol for chest radiography was selected in a standing position. The Source-to-Image Distance (SID) was fixed at 180 cm. For each patient category, the tube voltage (kV) was initially selected according to the established clinical protocol. A baseline exposure was then performed under these reference conditions.

Subsequently, for each patient category and for each of the three predefined thoracic thicknesses, additional exposures were acquired. These were carried out by systematically increasing and decreasing the tube voltage (kV) by 5kV, relative to the baseline setting. During all exposures, the tube current-time product (mAs) and the Exposure Index (EI) were recorded.

CNR and SNR calculation

For a quantitative evaluation of image quality, a calculation of Contrast-to-Noise Ratio (CNR) and Signal-to-Noise Ratio (SNR) was conducted. These metrics were derived as follows:

$$CNR = \frac{|MPV - MPV_{bg}|}{\sqrt{\frac{SD^2}{2} + \frac{SD_{bg}^2}{2}}} [16]$$

$$SNR = \frac{MPV}{SD} [17]$$

Where:

- MPV is the mean pixel value from a circular ROI derived from the area of the tenth circular disk from each acquired image.
- MPVbg is the mean pixel value from a circular ROI derived from the background area.
- SD and SDbg are the standard deviations of the measurements.
- In addition, the number of resolvable detail patterns of the Leeds test object was recorded as a qualitative indicator of spatial resolution.

ESD calculation

Entrance Surface Dose (ESD) was calculated using Air Kerma measurement. The measurement was conducted using), OCEAN software (RTI Electronics AB, Sweden) together with Piranha X-ray meter (RTI Electronics AB, Sweden) [16] with serial No. BC1- 05120015 that measures voltage, dose, dose rate, time and half-wavelength, calibrated on 14.03.2017, by Greek Atomic Energy Commission (EEAE).

The meter was placed on the radiography table at 100 cm SID (Source-Image Receptor Distance), using 15×15 cm^2 field. Exposure parameters used were 115 kV and 2mAs.

For the ESD calculation the following formula was implemented:

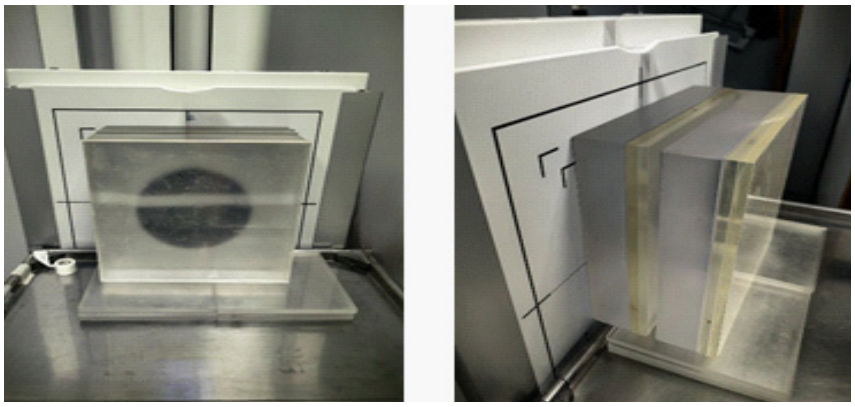

Figure 1: Measurement setup.

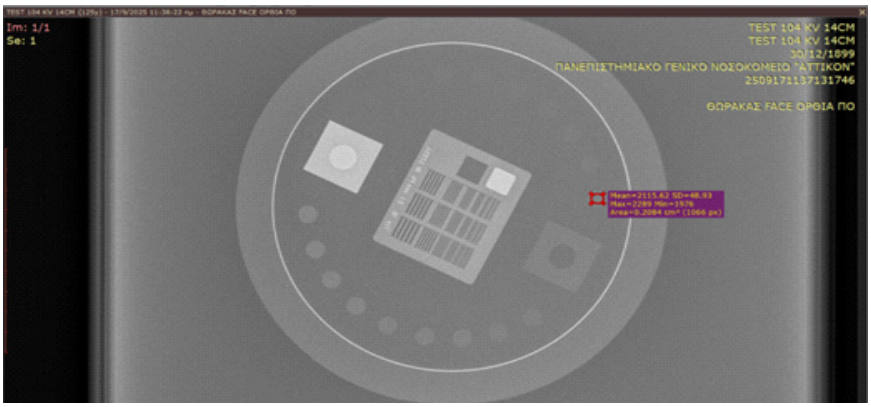

Figure 2: Leeds TOR 18FG image selection, MPV and SD evaluation.

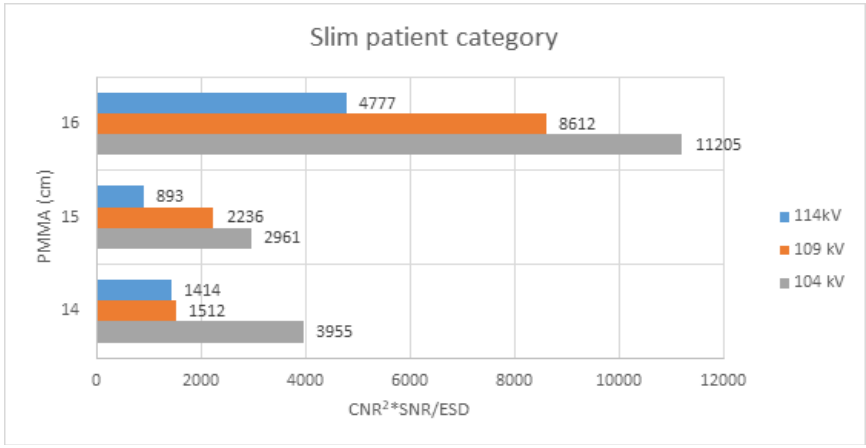

Figure 3: Bar graph of quality index ($CNR^2 \times SNR/ESD$) for the slim patient category as a function of PMMA thickness at three different tube voltages (104 kV, 109 kV, and 114 kV).

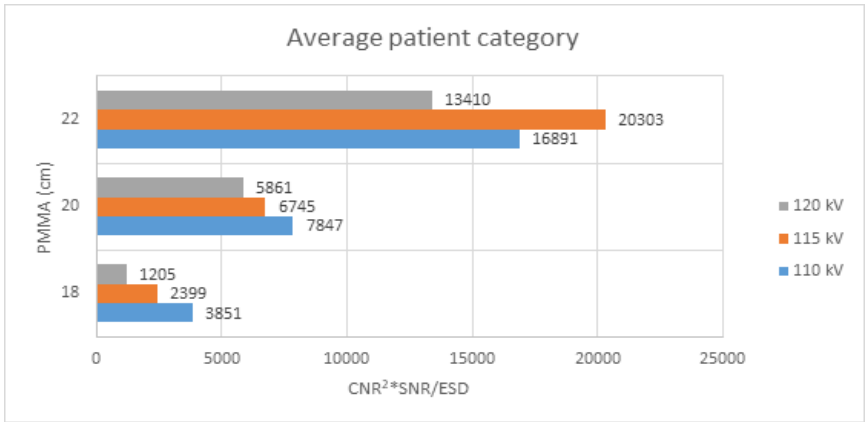

Figure 4: Bar graph of quality index ($CNR^2 \times SNR/ESD$) for the obese patient category as a function of PMMA thickness at three different tube voltages (116 kV, 121 kV, and 126 kV).

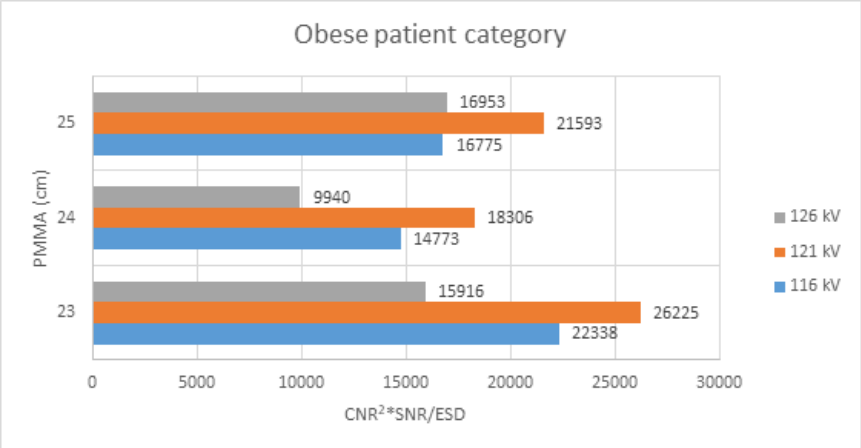

Figure 5: Bar graph of quality index ($CNR^2 \times SNR/ESD$) for the average patient category as a function of PMMA thickness at three different tube voltages (110 kV, 115 kV, and 120 kV).

Table 1: Data for slim patient category.

Slim Patient category											
kV	**mAs**	**d (cm)**	**EI**	**MPV**	**MPVbg**	**SD**	**SDbg**	**SNR**	**CNR**	**ESD (mGy)**	**CNR2·SNR/ESD**
104	3.7	14	215	2525.69	2421.13	57.75	49.49	43.73489	1.94426	0.042	3955
	4.2	15	208	2494.22	2406.24	60.43	47	41.27453	1.625253	0.037	2961
	4.8	16	193	2541.03	2394.76	56.91	45.31	44.64997	2.843615	0.032	11205
109	3.1	14	214	2521.57	2441.36	62.47	52.8	40.36449	1.386818	0.051	1512
	3.6	15	207	2469.56	2395.74	53.22	47.79	46.40286	1.45953	0.044	2236
	4	16	192	2556.29	2411.98	56.35	48.36	45.36451	2.748385	0.040	8612
114	2.7	14	51	2496.26	2400.02	62.06	56.02	40.22333	1.627953	0.075	1414
	3.2	15	48	2466.51	2406.23	58.48	44.46	42.17698	1.160454	0.064	893
	3.5	16	189	2531.81	2394.26	58.93	48.79	42.96301	2.542603	0.058	4777

Table 2: Data for average patient category.

Average Patient category											
kV	**mAs**	**d (cm)**	**EI**	**MPV**	**MPVbg**	**SD**	**SDbg**	**SNR**	**CNR**	**ESD (mGy)**	**CNR2·SNR/ESD**
110	5.1	18	170	2096.16	2170	47.68	42.8	43.96309	1.629815	0.030	3851
	6.5	20	148	2172.73	2273.55	49.95	47.34	43.4981	2.071821	0.024	7847
	8	22	56	2269.12	2410.93	53.25	49.12	42.61258	2.768286	0.019	16891
115	4.4	18	167	2088.21	2156.89	50.35	44.42	41.47388	1.446575	0.036	2399
	5.6	20	56	2165.79	2259.97	46.87	45.6	46.20845	2.036793	0.028	6745
	6.8	22	56	2255.51	2402.68	48.39	43.67	46.61108	3.193069	0.023	20303
120	3.7	18	160	2091.25	2157.52	54.03	47.02	38.70535	1.308483	0.055	1205
	4.7	20	53	2179.51	2288.37	47.23	45.6	46.14673	2.345001	0.043	5861
	5.7	22	71	2245.88	2401.12	48.54	47.98	46.26864	3.216689	0.036	13410

$$ESD = K_{air} \cdot \left(\frac{d_{ref}}{d_{FSD}} \right)^2 .a_{bsc} . \frac{mAs_{ref}}{mAs_m} [18]$$

where:

- Kair: Air Kerma,
- dref: Reference distance of the measurement (100 cm),
- dFSD: Focus Surface Distance,
- absc: Back scattering coefficient (1.35),
- mAsref: The tube current used in this measurement (2mAs) and
- mAsm: The tube current used for each study measurement.

Table 3: Data for obese patient category.

Obese patient category											
kV	mAs	d (cm)	EI	MPV	MPVbg	SD	SDbg	SNR	CNR	ESD (mGy)	CNR2·SNR/ESD
116	7.3	23	55	2284.68	2438.84	48.39	48.99	47.21389	3.166093	0.021	22338
	8.4	24	113	2337.94	2451.56	49.27	45.57	47.45159	2.394214	0.018	14773
	9.2	25	103	2373.73	2496.38	49.79	51.06	47.67483	2.432132	0.017	16775
121	6.2	23	114	2246.03	2434.35	48.63	50.01	46.1861	3.817956	0.026	26225
	7.2	24	110	2330.56	2467.02	46.35	49.79	50.28177	2.836961	0.022	18306
	7.9	25	100	2361.27	2500.15	47.05	47.29	50.1864	2.944235	0.020	21593
126	5.3	23	77	2277.37	2445.64	47.6	46.56	47.84391	3.573911	0.038	15916
	6.1	24	107	2331.43	2443.31	45.39	42.63	51.3644	2.540901	0.033	9940
	6.7	25	98	2367.91	2511.07	45.15	46.22	52.4454	3.133418	0.030	16953

Results

(Table 1) through 3 present the experimental measurements obtained for the three patient categories. For each category, and across the three tube voltage values and various PMMA thicknesses, the tube current-time product (mAs) reported by the imaging system and the Exposure Index (EI) are documented. Furthermore, the Mean Pixel Value (MPV) and Standard Deviation (SD) were derived both from the designated region of interest and from the background in each acquired image. From these primary data, the Signal-to-Noise Ratio (SNR), the Contrast-to-Noise Ratio (CNR), and the Entrance Surface Dose (ESD) were subsequently calculated as described in the methodology. In addition, the quality index (CNR^2·SNR/ESD) was determined, which provides a composite measure of image quality by simultaneously incorporating contrast, noise, and patient dose.

In the slim patients, as in (Table 1), both SNR and CNR measurements were quite high even at lowered kV levels, which suggests that excellent image quality can be achieved while maintaining reduced dose levels. Remarkably, when the voltage dropped to 104 kV, SNR and CNR revealed balanced values, whereas the corresponding ESD was markedly less than that with higher voltages.

For the average patient category, as demonstrated in (Table 2), both SNR and CNR values demonstrated greater variability across the different tube voltage settings. Higher kV values resulted in enhanced image quality, but were consistently associated with an increase in patient dose.

For obese patient category, as reported in (Table 3), SNR and CNR values improved with increasing tube voltage, the corresponding ESD was particularly high.

In (Figure 3), for the thin patient group, the quality index is higher at 104 kV-5 kV above the current clinical use-for all PMMA thicknesses investigated. For the average patient category (Figure 4), the quality index is greater at the standard tube voltage for the largest PMMA thickness (22 cm) and at lower tube voltages for the thinner phantoms. In the obese patient category (Figure 5), the quality index is consistently higher at the standard tube voltage across all three PMMA thicknesses assessed.

Discussion

In the current study, our findings indicate that the ideal tube voltage differs significantly across patient groups, emphasizing the need for personalized acquisition settings instead of standardized clinical protocols.

In slim patients, lower tube voltages (104 kV) provided adequate image quality while keeping ESD low, agreeing with a general trend that lower kV techniques resulted in better image quality, [14] indicating that existing institutional protocols may result in unnecessarily high exposures for this group. For average patients, thinner phantoms achieved better outcomes with lower voltages, whereas thicker phantoms required voltages nearer to the standard clinical settings. In obese patients, higher voltages consistently enhanced SNR and CNR, but a substantial increase in ESD.

These results align with prior studies indicating that the relationship between tube voltage and diagnostic image quality is strongly influenced by patient size and the anatomical region being imaged [19]. For instance, Uffmann et al. [20] reported in a flat-panel chest radiography study that lower kVp (90 kVp) improved anatomical visibility compared to higher kVp when dose was kept constant, particularly in the lung fields. Likewise, Grewal et al. (2012) [6] showed that carefully optimized reductions in exposure parameters can preserve diagnostic image quality. Subsequent phantom tests revealed that while larger kVp does minimize entrance dose, it will decrease contrast unless additional beam filtration is added [21]. The patient thickness effect is also validated: Monte Carlo simulations illustrate that greater body size (20-28 cm) requires more kVp to maintain image quality, and digital radiography machines function better than computed radiography at equal exposure levels [21]. Optimisation specific to regions was also observed, with lung fields better CNR at lower kVp, whereas mediastinal and spinal regions are benefited by higher voltages [22]. Our findings are reflecting the same pattern, with lean patients having adequate diagnostic quality at lower kVp, whereas obese patients required higher kVp to maintain similar image adequacy.

Most studies in the literature recommend using an anthropomorphic chest phantom to optimize chest digital radiography [23-25]. In contrast, our study demonstrates that even with basic tools commonly available in any clinic, a straightforward initial assessment can be performed to refine acquisition parameters, improving patient imaging while minimizing radiation dose.

This study has several limitations that should be acknowledged. Although phantom measurements are widely practiced, the latter cannot fully simulate patient anatomy or tissue het-

erogeneity. Only tube voltage was manipulated systematically, while other determinants-such as beam filtration, grid use, or exposure time modulation-were not tested. The study was further performed on one DR system alone, limiting the generalizability of results to other manufacturers or detector technology. Future research must apply this methodology to clinical populations, ideally with the inclusion of observer performance studies or diagnostic accuracy outcomes.

Conclusion

In summary, we demonstrate through this study that chest radiography optimization should not be founded on an equal protocol but must take patient size and body habitus into consideration. Through a systematic evaluation of the relationship between image quality and radiation dose, we demonstrate that clinically significant reductions in patient exposure are indeed possible without compromising diagnostic performance, especially for thin and average patients.

Overall, these findings highlight a core principle in radiology: maximizing patient safety and diagnostic excellence depends on evidence-based, adaptable, and patient-tailored imaging protocols. When radiography adopts individualized optimization strategies, it can remain a vital component of medical care without burdening patients with undesirable risks.

References

1. Agency IAE. International Conference on Radiological Protection of Patients in Diagnostic and Interventional Radiology, Nuclear Medicine and Radiotherapy. IAEA.
2. Joarder R, N Crundwell. Chest X-Ray in Clinical Practice. 2009; 1-195.
3. Radiation, UNSCotEoA. Sources and effects of ionizing radiation.
4. Kamposioras K, et al. Screening chest radiography: results from a Greek cross-sectional survey. BMC Public Health. 2006; 6: 113.
5. Proiskos A, et al. Screening chest radiography in primary care: An underestimated belief. The European journal of general practice. 2005; 11: 76-7.
6. Grewal RK, et al. Digital chest radiography image quality assessment with dose reduction. Australas Phys Eng Sci Med. 2012; 35(1): 71-80.
7. Suliman II, SO Elawed. Radiation dose measurements for optimisation of chest X-ray examinations of children in general radiography hospitals. Radiat Prot Dosimetry. 2013; 156(3): 310-4.
8. Nekolla EA, et al. Frequency and doses of diagnostic and interventional X-ray applications: Trends between 2007 and 2014. Radiologe. 2017; 57(7): 555-562.
9. Regulla DF, H Eder. Patient exposure in medical X-ray imaging in Europe. Radiation Protection Dosimetry. 2005; 114(1-3): 11-25.
10. Samara ET, et al. Exposure of the swiss population by medical x-rays: 2008 review. Health Physics. 2012; 102(3).
11. De González AB, S Darby. Risk of cancer from diagnostic X-rays: Estimates for the UK and 14 other countries. The Lancet. 2004; 363(9406): 345-351.
12. Tschauner S, et al. European Guidelines for AP/PA chest X-rays: Routinely satisfiable in a paediatric radiology division? Eur Radiol. 2016; 26(2): 495-505.
13. Australia MRPBo. Code of Conduct for Medical Radiation Practitioners. 2014.
14. Steffensen C, et al. Optimisation of radiographic acquisition parameters for direct digital radiography: A systematic review. Radiography (Lond). 2021; 27(2): 663-672.
15. DR 600 Ceiling. Available from: https://agfaradiologysolutions.com/products/dr-600/.
16. Kordolaimi SD, et al. Comparative performance evaluation of a flat detector and an image intensifier angiographic system both used for interventional cardiology procedures in adult and pediatric patients. Physica Medica. 2013; 29(2): 178-187.
17. Konstantinidis A. 2.02 - Physical Parameters of Image Quality, in Comprehensive Biomedical Physics, A. Brahme, Editor. 2014; 49-63.
18. Alomairy N, et al. Evaluation of the Entrance Surface Doses (ESD) for common diagnostic X-ray examinations. Journal of Radiation Research and Applied Sciences. 2023; 16(4): 100754.
19. Welarathna S, S Velautham, S Sarasanandarajah. Patient-size based dose optimization in projection radiography examinations: A BMI-guided approach. J Appl Clin Med Phys. 2025; 26(7): e70191.
20. Uffmann M, et al. Flat-panel-detector chest radiography: effect of tube voltage on image quality. Radiology. 2005; 235(2): 642-50.
21. Ullman G, et al. The influence of patient thickness and imaging system on patient dose and physical image quality in digital chest imaging. Radiat Prot Dosimetry. 2005; 114(1-3): 294-7.
22. Moore CS, AW Beavis, JR Saunderson. Investigation of optimum X-ray beam tube voltage and filtration for chest radiography with a computed radiography system. Br J Radiol. 2008; 81(970): 771-7.
23. Vassileva J. A phantom approach to find the optimal technical parameters for plain chest radiography. Br J Radiol. 2004; 77(920): 648-53.
24. Pengpan T, et al. Optimization of Image Quality and Organ Absorbed Dose for Pediatric Chest X-Ray Examination: In-House Developed Chest Phantom Study. Radiol Res Pract. 2022; 2022: 3482458.
25. Vassileva J. A phantom for dose-image quality optimization in chest radiography. Br J Radiol. 2002; 75(898): 837-42.